Fourier transform infrared emission spectroscopy and *ab initio* calculations on RuN

R. S. Ram[a)]
Department of Chemistry, University of Arizona, Tucson, Arizona 85721

J. Liévin
Université Libre de Bruxelles, Laboratoire de Chimie Physique Moléculaire, CP 160/09, Av. F. D. Roosevelt 50, Bruxelles, Belgium

P. F. Bernath
Department of Chemistry, University of Arizona, Tucson, Arizona 85721; Université Libre de Bruxelles, Laboratoire de Chimie Physique Moléculaire, CP 160/09, Av. F. D. Roosevelt 50, Bruxelles, Belgium; and Department of Chemistry, University of Waterloo, Waterloo, Ontario, Canada N2L 3G1

(Received 4 June 1998; accepted 14 July 1998)

The emission spectrum of RuN has been observed in the near infrared using a Fourier transform spectrometer. RuN molecules were excited in a hollow cathode lamp operated with neon gas and a trace of nitrogen. Two bands with 0–0 Q heads near 7354 and 8079 cm^{-1} and a common lower state have been assigned as $^2\Pi_{1/2}-{}^2\Sigma^+$ and $^2\Pi_{3/2}-{}^2\Sigma^+$ subbands, respectively, of a $C\ ^2\Pi-X\ ^2\Sigma^+$ transition. A rotational analysis of these bands has been performed and molecular constants have been extracted. The principal molecular constants for the ground $X\ ^2\Sigma^+$ state of the most abundant ^{102}RuN isotopomer are: $B_0=0.552\ 782\ 9(70)\ cm^{-1}$, $D_0=5.515(13)\times10^{-7}\ cm^{-1}$, $\gamma_0=-0.044\ 432(22)\ cm^{-1}$ and $r_0=1.573\ 869(10)$ Å. The excited $C\ ^2\Pi$ state has the following molecular constants: $T_{00}=7714.342\ 60(53)\ cm^{-1}$, $A_0=725.8064(11)\ cm^{-1}$, $B_0=0.516\ 843\ 4(80)\ cm^{-1}$, $D_0=5.685(16)\times10^{-7}\ cm^{-1}$, $p_0=5.467(36)\times10^{-3}\ cm^{-1}$ and $r_0=1.627\ 670(13)$ Å. *Ab initio* calculations have been carried out on RuN to ascertain the nature of the experimentally observed states and to predict the spectroscopic properties of the low-lying electronic states. Our electronic assignment is supported by these calculations and is also consistent with the observations for the isoelectronic RhC molecule [Kaving and Scullman, J. Mol. Spectrosc. **32**, 475–500 (1969)]. The valence electron configuration $1\sigma^2 2\sigma^2 1\pi^4 1\delta^4 3\sigma^1$ is proposed for the $X\ ^2\Sigma^+$ ground state of RuN and the configurations for the excited states have been discussed. There is no previous experimental or theoretical work on RuN. © *1998 American Institute of Physics.* [S0021-9606(98)01339-7]

INTRODUCTION

In recent years, there has been growing interest in the study of transition metal-containing molecules because of their importance in astrophysics,[1,2] catalysis and organometallic chemistry.[3,4] Transition metal-containing diatomics have been the subject of many theoretical[5–8] and experimental studies[9–11] in order to understand the bonding in simple systems and, particularly, the interaction of transition metals with hydrogen, carbon, nitrogen, and oxygen.

Transition metal nitrides are important in the fixation of nitrogen in industrial, inorganic, and biological systems.[12,13] The Haber process for the synthesis of ammonia proceeds through the chemisorption of nitrogen on surfaces. The biological fixation of nitrogen involves an iron–molybdenum–sulfur cluster at the active site of molybdenum nitrogenase enzyme. Inorganic complexes of Mo and W can also fix nitrogen through dinitrogen complexes. The formation and nature of the metal–nitrogen bond is thus an active area of research with many applications.

Transition metal atoms are relatively abundant in cool M-and S-type stars[14] and several transition metal hydrides and oxides also have been detected.[15–19] Since transition metal nitrides and oxides often have similar bond energies, the nitrides are also of potential astrophysical importance. Although metal nitride molecules have not been observed yet in stellar atmospheres, they would provide valuable information on the abundance of nitrogen. Precise spectroscopic data are necessary for a meaningful search for these molecules in complex stellar spectra. The spectra of many transition metal hydrides and oxides have been well characterized (for example Refs. 20–25) in the last few years, in contrast to the nitrides and the carbides. Some recently studied nitrides are ScN,[26] YN,[27] HfN,[28] WN,[29] ReN,[30,31] RhN,[32] CrN,[33] PtN,[34,35] and IrN.[36] Theoretical calculations are also available, for example, for ScN,[37] YN,[38] TiN,[39–41] VN,[41,42] CrN,[41] and FeN.[43–45]

Among the possible Ru-containing diatomic molecules, spectra of RuO[46,47] and RuC[48] have been analyzed previously. In the present paper we report on the discovery of an infrared electronic transition of RuN recorded by high-resolution Fourier transform emission spectroscopy. Two bands observed at 7354 and 8079 cm^{-1} have been assigned

a)Electronic mail: rram@u.arizona.edu

as the 0–0 bands of the $C\ ^2\Pi_{1/2}-X\ ^2\Sigma^+$ and $C\ ^2\Pi_{3/2}-X\ ^2\Sigma^+$ subbands, respectively. Although no previous theoretical or experimental information is available for RuN to serve as a guide, the present assignments are consistent with the measurements made on the isoelectronic RhC molecule.[49,50] The TcO molecule is also isoelectronic with RuN but TcO is calculated to have a $^6\Sigma^+$ ground state.[51] In addition, FeN[45] and ReO,[31] which are isovalent with RuN, probably have $^2\Delta$ state ground states. In order to independently confirm our assignments, *ab initio* calculations have been performed on RuN and the spectroscopic properties of the low-lying electronic states have been predicted. These calculations are, in general, in good agreement with our infrared observations.

EXPERIMENT

RuN molecules were excited in a hollow cathode lamp and the spectra were recorded with the 1 m Fourier transform spectrometer associated with the McMath–Pierce Solar Telescope of the National Solar Observatory at Kitt Peak. The cathode was prepared by pressing a mixture of Ru and Cu metal powder (1:3 ratio) in a 10 mm diameter hole in a copper block. After completely filling the hole, the block was bored through to give an 8 mm diameter hole in the center. This procedure provided an ~1 mm thick layer of the Cu–Ru mixture on the inner wall of the cathode. The lamp was operated at 600 mA and 350 V current with a slow flow of 2.5 Torr of Ne carrier gas. The new bands appeared when a trace of N_2 (~6 mTorr) was added to the neon flow and disappeared when N_2 was replaced by O_2, suggesting that the new bands were indeed due to RuN.

The spectra from 1800 to 9000 cm^{-1} were recorded using InSb detectors and silicon filters with 14 scans co-added in about 90 min of integration. In addition to the RuN bands, the observed spectra also contained Ru and Ne atomic lines as well as N_2 molecular lines. The spectra were calibrated using the measurements of Ne atomic lines made by Palmer and Engleman.[52]

The spectral line positions were extracted from the observed spectra using a data reduction program called PC-DECOMP developed by J. Brault. The peak positions were determined by fitting a Voigt line shape function to each spectral feature. The branches in the different subbands were sorted using a color Loomis–Wood program running on a PC computer. The absolute accuracy of the wave number scale is expected to be of the order of ± 0.003 cm^{-1}. The strong lines of RuN appear with a typical signal to noise ratio of 15:1 and have a typical line width of about 0.045 cm^{-1}. The precision of measurements of strong and unblended RuN lines is expected to be better than ± 0.003 cm^{-1}.

AB INITIO CALCULATIONS

Ab initio calculations were performed on RuN with the internally contracted multireference configuration interaction method (CMRCI)[53] for the low-lying states of doublet, quartet, and sextet spin multiplicities. These CMRCI calculations were preceded by complete active space self-consistent field (CASSCF) calculations[54] in which all valence molecular orbitals were optimized. The lowest energy states of Σ^+, Π, Δ, and Φ symmetry have been calculated for each spin multiplicity, except in the doublet manifold where two Π and Φ states arising from the same configuration were considered (see below). All calculations were performed with the MOLPRO96 program package,[55] running on the Cray J916 computer at the ULB/VUB computer center.

The quasi relativistic *ab initio* pseudo potential developed in Stuttgart by Andrae *et al.*[56] has been used to represent the core electrons of the ruthenium atom, together with the corresponding valence-optimized orbital basis set. For nitrogen, we have also used, for sake of consistency, a pseudo potential and the corresponding basis set developed along the same lines.[57] The parameters of the pseudo potentials have been energy-adjusted in a least-squares fit to the valence energies of several neutral and ionic atomic states. The valence energies were obtained from quasi relativistic Wood–Boring (WB) calculations,[58] in which the major relativistic corrections, i.e., the mass-velocity and the Darwin-spin–orbit terms, were taken into account. For second row ($4d$) transition metal atoms, Andrae *et al.*[56] have considered the valence space to include the $4s$, $4p$, $4d$, and $5s$ orbitals, thus leaving 28 electrons in the core. This definition of the core-valence separation is justified[56] on the basis of extensive experience with transition metal core-potential calculations. The usual definition of a $1s$ core orbital was adopted for nitrogen. The valence orbitals of Ru are expanded on ($8s$ $7p$ $6d$) primitive Gaussian functions, contracted to [$6s$ $5p$ $3d$]. We have added a single $4f$ orbital to this standard basis set, with a Gaussian exponent of 0.8, optimized in CASSCF calculations performed on RuN at the equilibrium geometry. For nitrogen, the ($4s$ $4p$) primitive basis set was contracted to double-zeta [$2s$ $2p$] and augmented by a single $3d$ polarization function with an exponent of 0.8.

The active orbital space[59] used in the CASSCF calculations, to be considered throughout this work as the valence space of RuN, is defined by the molecular orbitals correlating with the $4d$ and $5s$ orbitals of ruthenium and the $2s$ and $2p$ orbitals of nitrogen, leading to one δ, two π, and four σ valence orbitals. All possible configuration state functions (CSFs) arising from the distribution of the corresponding 13 valence electrons within this active space have been included in the CASSCF calculations. The two σ orbitals and the single π orbital arising from the $4s$ and $4p$ orbitals of ruthenium, not included in the core potential as explained above, were defined as closed shells in all CSFs, which means that they were optimized by the MCSCF procedure, but not explicitly correlated. One can thus consider that all dynamical correlation effects within the defined valence space have been accounted for in our CASSCF calculations. These calculations have served as a preliminary orbital optimization step to prepare for the CMRCI calculations. A state-averaging procedure has been used in order to optimize, at each different geometry, a common molecular orbital basis set for describing the low-lying states of a given spin multiplicity.

The multireference wave function used in the CMRCI calculations exactly corresponds to the CASSCF wave function. All single and double electron replacements from the

valence orbitals to the external orbital space were included in the CMRCI expansion. This level of calculation is expected to take into account both dynamical and nondynamical correlation effects. The CMRCI energies were also corrected for Davidson's contribution[60] from unlinked four-particle clusters.

Some orders of magnitude for the size of the *n*-electron basis sets used in our calculations are given below. The CASSCF (CMRCI) wave functions are expanded with about 3500 (400 000) CSFs for doublet states, 2300 (353 000) CSFs for quartet states, and 500 (145 000) CSFs for sextet states. These numbers refer to CSFs expansions expressed within the C_{2v} point symmetry group, given the inherent symmetry used in MOLPRO.[55] The internal contraction technique implemented in this program allows for deep reductions of the configurational spaces without a significant loss of accuracy.[53] For instance, the CMRCI calculations that we have performed on the doublet states of RuN involve about 400 000 contracted CSFs, although the corresponding uncontracted calculation would have included more than 16 million of CSFs.

OBSERVATION AND ANALYSIS

RuN bands are located in the 5500–9500 cm^{-1} region. The two strong bands located near 7354 and 8079 cm^{-1} have been assigned as the 0–0 bands of the $^2\Pi_{1/2}-^2\Sigma^+$ and $^2\Pi_{3/2}-^2\Sigma^+$ subands of the $C\ ^2\Pi-X\ ^2\Sigma^+$ transition of RuN. There are a few very weak bands located near 6155, 6971, 7251, 8360, and 9076 cm^{-1} that seem to involve higher vibrational levels. The bands near 6971 and 9076 cm^{-1} are most probably the 0–1 and 1–0 bands of the $^2\Pi_{3/2}-^2\Sigma^+$ subband providing $\Delta G''_{1/2}=1108\ cm^{-1}$ and $\Delta G'_{1/2}=997\ cm^{-1}$. In the $^2\Pi_{1/2}-^2\Sigma^+$ subband there is a very strong atomic line in the vicinity of the 0–1 band and the assignment of the lower state vibrational interval cannot be confirmed independently. A very weak band at 8360 cm^{-1} is most probably the 1–0 band the $^2\Pi_{1/2}-^2\Sigma^+$ subband providing $\Delta G'_{1/2}=1006\ cm^{-1}$. Although the 0–1 band is obscured by a very strong atomic line, weak features at 7251 and 6155 cm^{-1} are at the correct positions of the 1–1 and 1–2 bands of the $^2\Pi_{1/2}-^2\Sigma^+$ subband. If this is the case, the $^2\Pi_{1/2}-^2\Sigma^+$ subband gives $\omega_e=1122$ and $\omega_e x_e=6.5\ cm^{-1}$ in the ground state. The position of the weaker band heads could be in error by as much as $\pm 2\ cm^{-1}$. In addition to RuN bands there are several N_2 bands spread through out the spectrum. In spite of this overlapping, the strong RuN bands can be clearly distinguished from N_2 on the basis of the spacing between consecutive rotational lines. Luckily the $^2\Pi_{1/2}-^2\Sigma^+$ subband is free from overlap and only 40 cm^{-1} of the $^2\Pi_{3/2}-^2\Sigma^+$ 0–0 band (near the head) is overlapped by an N_2 band which is degraded towards high wave numbers. A few badly overlapped lines were not included in the analysis.

A portion of the compressed spectrum of the $C\ ^2\Pi_{1/2}-X\ ^2\Sigma^+$ 0–0 band is presented in Fig. 1. Each band is double headed and consists of six branches. At first glance the spectrum looks complex, particularly at higher *J*, because of resolved isotopic splittings. A section of the

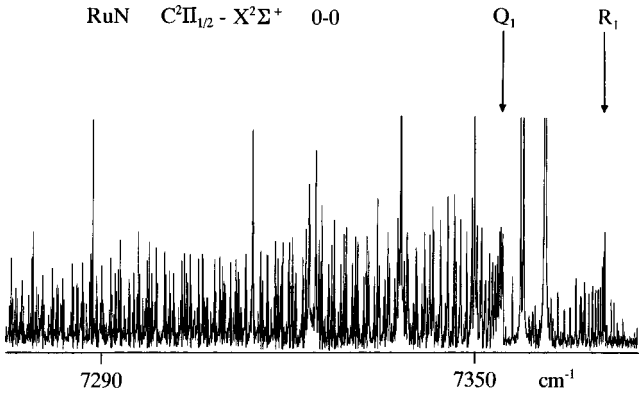

FIG. 1. A compressed portion of the 0–0 band of the $C\ ^2\Pi_{1/2}-X\ ^2\Sigma^+$ subband of RuN.

$C\ ^2\Pi_{1/2}-X\ ^2\Sigma^+$ 0–0 band located about 60 cm^{-1} below the band origin is presented in Fig. 2 to illustrate the isotope effect. The lines in all of the branches were picked out using our color Loomis–Wood program. Ruthenium has seven naturally occurring isotopes ^{96}Ru(5.5%), ^{98}Ru(1.9%), ^{99}Ru(12.7%), ^{100}Ru(12.6%), ^{101}Ru(17.0%), ^{102}Ru(31.6%), and ^{104}Ru(18.7%). The three lines marked for each *J* in Fig. 2 are due to the ^{100}RuN, ^{102}RuN, and ^{104}RuN isotopomers since the ^{100}Ru, ^{102}Ru, and ^{104}Ru nuclei all have zero nuclear spin and are abundant. ^{99}Ru and ^{101}Ru nuclei also have significant abundance but they have the high nuclear spin of $\frac{5}{2}$ so that the ^{99}RuN and ^{101}RuN lines are expected to be split into six hyperfine components. The ^{99}RuN and ^{101}RuN lines would not be seen in our spectra at the present resolution and signal-to-noise ratio. We have rotationally analyzed only the most abundant ^{102}RuN lines which are located in the center of the isotopic pattern (Fig. 2). The rotational assignment of the two subbands was made by comparing the lower state combination differences. The ^{102}RuN line positions in the 0–0 band of the $C\ ^2\Pi-X\ ^2\Sigma^+$ transition are available from PAPS[61] or from the authors upon request.

The fit of the observed lines was obtained utilizing the effective Hamiltonian of Brown *et al.*[62] The matrix elements

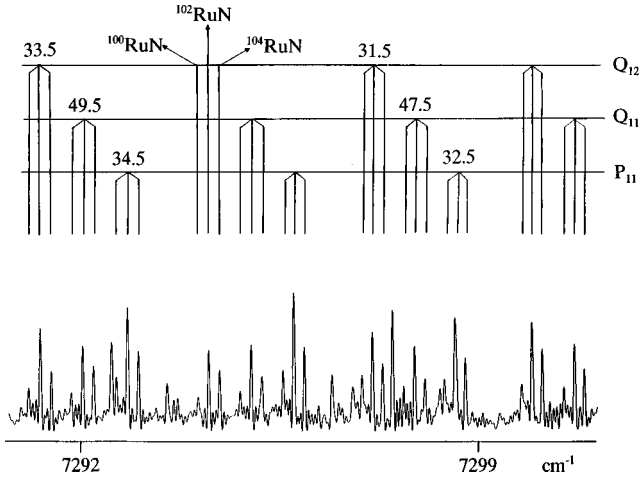

FIG. 2. A portion of high *J* lines of the 0–0 band of the $C\ ^2\Pi_{1/2}-X\ ^2\Sigma^+$ subband of RuN with some lines of ^{100}RuN, ^{102}RuN, and ^{104}RuN isotopomers marked.

TABLE I. Spectroscopic constants (in cm^{-1}) for ^{102}RuN from a fit where the two excited states were treated as spin components of a case (a) $^2\Pi$ state.

Constants[a]	$X\ ^2\Sigma^+$	$C\ ^2\Pi$
T_0	0.0	7714.342 60(53)
A_0	⋯	725.8064(11)
$10^3\times A_{D0}$	⋯	−1.2815(41)
$10^7\times A_{H0}$	⋯	−1.556(21)
B_0	0.552 782 9(70)	0.516 843 4(80)
$10^7\times D_0$	5.515(13)	5.685(16)
$10^{11}\times H_0$	⋯	−1.849(12)
γ_0	−0.044 432(22)	⋯
$10^4\times \gamma_{D0}$	−0.002 031(54)	−1.510(20)
$10^8\times \gamma_{H0}$	⋯	1.600(11)
$10^3\times p_0$	⋯	5.467(36)
$10^6\times p_{D0}$	⋯	1.4527(83)

[a]Numbers in parentheses are one standard deviation in the last two digits.

for a $^2\Sigma$ Hamiltonian are listed by Douay *et al.*[63] and those for a $^2\Pi$ state are provided by Amiot *et al.*[64] In the beginning of the analysis, the two subbands were fitted separately and it was noted that the lower state constants from the two fits were very similar, as expected. Next an attempt was made to fit both of the subbands together, with the $C\ ^2\Pi$ state treated as a Hund's case (a) state. A large number of higher order constants were required in the excited state in order to minimize the standard deviation of the fit. For the ground state the rotational constants B_0, D_0, γ_0, and γ_{D0} were determined in this fit, as well as in the separate fits. In the excited state, however, higher order constants such as A_{D0}, A_{H0}, γ_{D0}, and γ_{H0} were also required in addition to usual T_0, A_0, B_0, D_0, H_0, p_0, and p_{D0} constants (Table I). The excited $C\ ^2\Pi$ state has a large spin–orbit splitting of 725.8 cm^{-1} and the two spin components are clearly interacting in a global way with nearby electronic states. These interactions are also reflected in, for example, the anomalous relative values of the effective B constants for each spin component seen in the separate subband fits, consistent with some Hund's case (c) behavior (Table II). Local perturbations in both parity levels at the same J were also found in the $C\ ^2\Pi_{1/2}$ spin component near $J'=41.5$. This observation also proves that there are other interacting states located in the vicinity of the excited $C\ ^2\Pi$ state and that the determination of higher order constants A_D, A_H, γ_D, and γ_H is just

TABLE II. Spectroscopic constants (in cm^{-1}) for ^{102}RuN from a fit where the two excited state spin components were treated as independent states.

Constants[a]	$X\ ^2\Sigma^+$	$C\ ^2\Pi_{1/2}$	$C\ ^2\Pi_{3/2}$
T_0	0.0	7714.337 96(66)	7714.344 78(69)
A_0	⋯	725.8064[b]	725.8064[b]
B_0	0.5527890(65)	0.517 742 1(64)	0.516 272 6(68)
$10^7\times D_0$	5.531(12)	5.831(12)	6.158(16)
$10^{12}\times H_0$	⋯	−4.193(49)	−0.3057(19)
γ_0	−0.044407(20)	⋯	⋯
$10^7\times \gamma_{D0}$	−2.116(50)	⋯	⋯
$10^3\times p_0$	⋯	5.529(33)	⋯
$10^5\times p_{D0}$	⋯	0.143 94(78)	−1.37(22)

[a]Numbers in parentheses are one standard deviation in the last two digits.
[b]Fixed to the value obtained in case (a) fit of the $C\ ^2\Pi$ state.

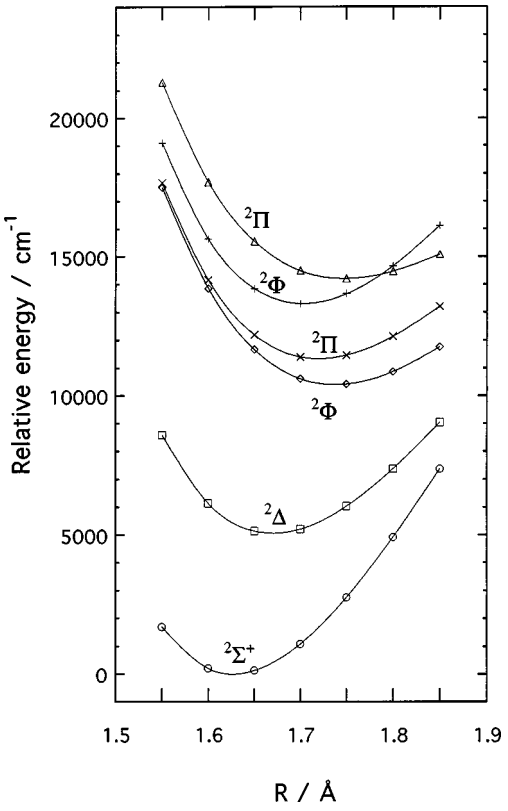

FIG. 3. The low-lying doublet potential-energy curves of RuN.

a reflection of these interactions. In order to extract a set of constants which accurately represent the energy levels of the two spin components, another fit was obtained in which the $^2\Pi_{1/2}$ and $^2\Pi_{3/2}$ excited spin components were treated as separate states with A_0 fixed to 725.8064 cm^{-1} (from the combined fit). The constants obtained from this fit are provided in Table II.

AB INITIO RESULTS

The potential-energy curves calculated at the CMRCI level of theory are shown in Figs. 3, 4, and 5, for the doublet, quartet, and sextet spin multiplicities, respectively. The energy scale used in these figures is relative to the minimum of the ground electronic state, which is predicted to be of $^2\Sigma^+$ symmetry ($X\ ^2\Sigma^+$). The low-lying excited states in the doublet manifold are: $A\ ^2\Delta$, $B\ ^2\Phi$, $C\ ^2\Pi$, $D\ ^2\Phi$, and $E\ ^2\Pi$ states. The quartet and sextet manifolds are shifted to higher energies, as better illustrated in Fig. 6, which reproduces the term energies of the different spin manifolds on a common energy scale.

The correlation diagrams drawn in Fig. 7 and 8 allow for a simple interpretation of the ordering of the electronic states as predicted by our CMRCI calculations. Figure 7 correlates the molecular orbitals of RuN to those of the ruthenium and nitrogen atoms in their ground states. This diagram has been obtained from size-consistent full-valence CASSCF calculations performed on RuN, Ru (^5F), and N (^4S). The RuN orbitals were obtained from a state-averaged CASSCF calculation performed at 1.65 Å on the low-lying doublet states,

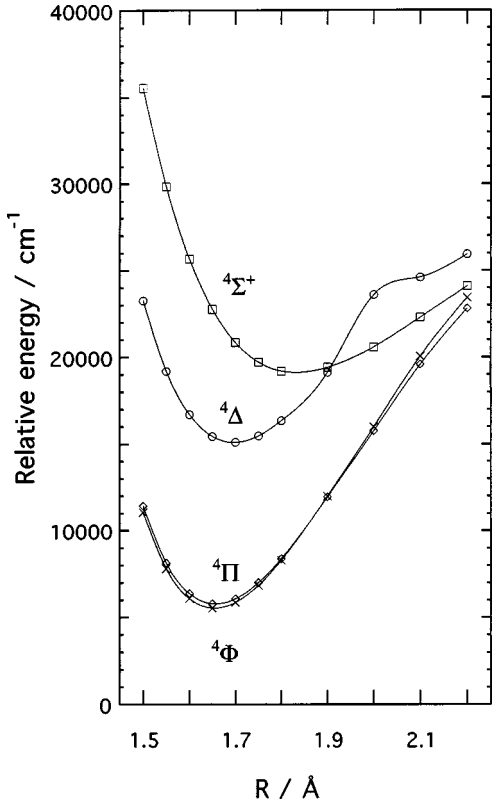

FIG. 4. The low-lying quartet potential-eergy curves of RuN.

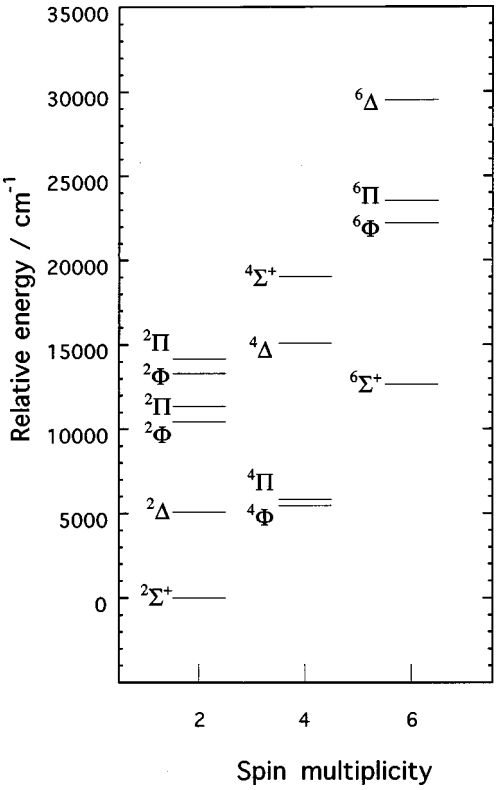

FIG. 6. The low-lying energy levels of RuN.

from $X\ ^2\Sigma^+$ to $E\ ^2\Pi$. All these states correlate to the lowest dissociation limit $\mathrm{Ru}(^5F)+\mathrm{N}(^4S)$. The resulting averaged orbitals provide a helpful one-electron picture for discussing the electron configuration ordering within the doublet manifold. The electron orbital filling represented in Fig. 7, with the 13 valence electrons distributed in the low-lying orbitals, predicts the ground configuration to be

$$1\sigma^2 2\sigma^2 1\pi^4 1\delta^4 3\sigma^1 (X\ ^2\Sigma^+).$$

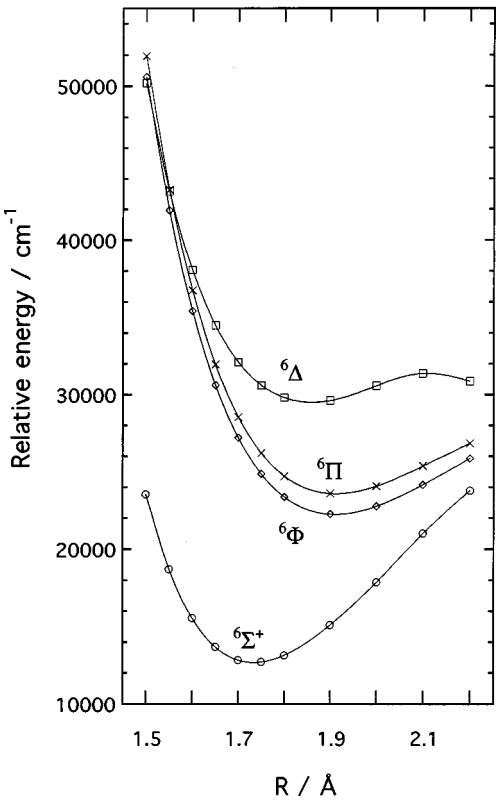

FIG. 5. The low-lying sextet potential-energy curves of RuN.

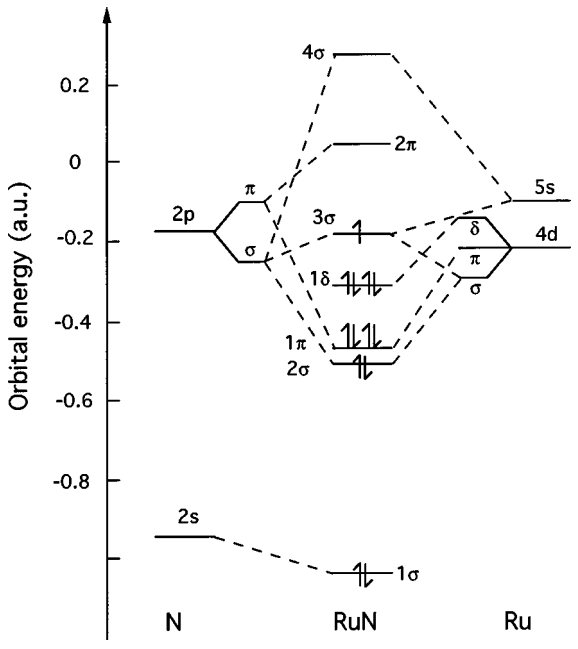

FIG. 7. The molecular-orbital correlation diagram for RuN.

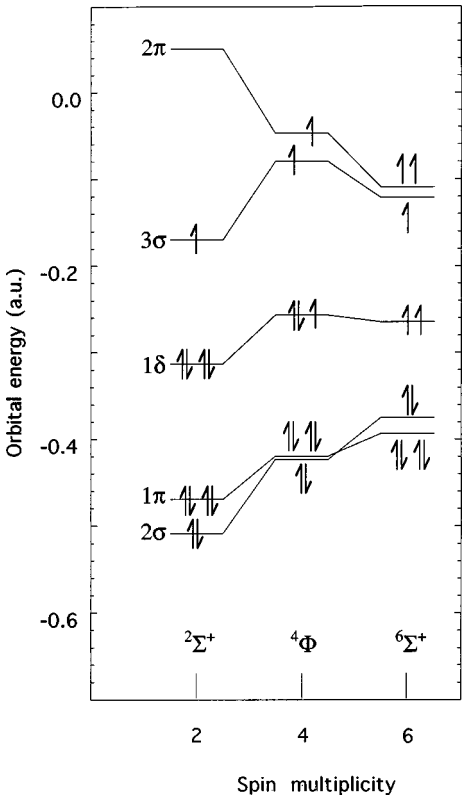

FIG. 8. The change in effective orbital energies as the spin multiplicity changes in RuN.

This prediction is in agreement with the analysis of the corresponding CMRCI wave function provided in Table III, in which are listed the main configurations contributing to the CI (configuration interaction) expansion, together with their weights in the CI wave function. The configuration weights are given by the square of the corresponding CI coefficients. One sees that all calculated states are characterized by a single dominant configuration, having a weight ranging between 60% and 80%, indicative of extensive configuration mixing. In most cases the second dominant weight is quite small and the remaining contributions are distributed over a large number of configurations. These features demonstrate the existence of strong electron correlation effects, as expected in such a system. We note that for some states, there are non-negligible contributions from configurations that open the internal 2σ orbital in order to occupy the antibonding 4σ orbital. We have further studied the correlation effects arising from the 1σ and 2σ orbitals. CMRCI test calculations demonstrate that restricting the internal space by excluding these two orbitals from the set of correlated orbitals, causes important effects. The state ordering is dramatically changed: Namely the first and second excited states, of $^2\Delta$ and $^2\Pi$ symmetry, respectively, become quasi-degenerate, which is far from the case at a higher level of theory (see Fig. 3).

Going back to Fig. 7, one can verify that a 1δ to 3σ electron promotion is consistent with the analysis of the $A^2\Delta$ wave function,

$$1\sigma^2 2\sigma^2 1\pi^4 1\delta^3 3\sigma^2(A^2\Delta).$$

The next most stable configuration predicted from the correlation diagram should arise from the 3σ to 2π excitation

$$1\sigma^2 2\sigma^2 1\pi^4 1\delta^4 2\pi^1(^2\Pi),$$

but it appears (see Table III) that the following configuration is more stable:

$$1\sigma^2 2\sigma^2 1\pi^4 1\delta^3 3\sigma^1 2\pi^1[^2\Pi(2),^2\Phi(2)].$$

We thus assign the experimentally observed transition as

$$1\sigma^2 2\sigma^2 1\pi^4 1\delta^3 3\sigma^1 2\pi^1(C\ ^2\Pi)$$
$$\rightarrow 1\sigma^2 2\sigma^2 1\pi^4 1\delta^4 3\sigma^1(X\ ^2\Sigma^+).$$

The dotted lines (Fig. 7) connecting the orbitals of RuN to those of the atomic dissociation products also give some interesting qualitative information on the atomic orbital content of the RuN molecular orbitals. These lines indicate the atomic orbitals that are actually mixed in the RuN orbitals, as given from an analysis of the CASSCF wave functions. One finds that:

(i) The 2σ and 3σ MOs are, respectively, constructed from bonding and antibonding combinations of $4d\sigma$(Ru) and $2p\sigma$(N);
(ii) 3σ has in addition some $5s\sigma$(Ru) $-$ $2p\sigma$(N) bonding character;
(iii) 1π and 2π, respectively, come from bonding and antibonding combinations of $4d\pi$(Ru) and $2p\pi$(N);
(iv) 4σ is the antibonding analog of 3σ.

Figure 8 presents a correlation diagram between the different spin systems. Following the philosophy adopted for Fig. 7, we have performed state-averaged CASSCF calculations on the lowest states of Σ^+, Π, Δ, and Φ symmetry for each spin multiplicity. One can expect in this way a consistent orbital energy scale within and between the spin manifolds. The most stable electron distributions have been drawn on this figure for each multiplicity. The doublet system has already been discussed. The one-electron picture for the quartets and sextets gives as lowest energy configurations and states

$$1\sigma^2 2\sigma^2 1\pi^4 1\delta^3 3\sigma^1 2\pi^1(^4\Phi)$$

and

$$1\sigma^2 2\sigma^2 1\pi^4 1\delta^2 3\sigma^1 2\pi^2(^6\Sigma^+).$$

This again agrees with the CMRCI wave function analysis (see Table III). One can verify that the excited configurations obtained by single electron promotions also match the calculated excited state ordering.

Let us also remark that Fig. 8 clearly indicates that most orbital energies undergo destabilization with increasing spin multiplicity, which confirms the energy shifts observed in Fig. 6. The 2π orbital exhibits, however, the opposite trend and becomes more stable as it becomes occupied.

The spectroscopic properties calculated from the CMRCI potential-energy curves are given in Table IV for the equilibrium internuclear distances r_e, the harmonic frequencies at equilibrium ω_e, and the term energies T_0, corrected for the zero-point energy contribution calculated within the harmonic approximation.

TABLE III. Weights of the main configurations[a] in the low-lying electronic states of RuN, from an analysis of the MRCI wave functions.

State[b]	Configurations[c]							Configuration weights (%)
	1σ	2σ	1π	1δ	3σ	2π	4σ	
$^2\Sigma^+$	2	2	4	4	1			75
	2	2	3	4	1	1		2
	2	2	2	4	1	2		6
	2	1	3	4	1	1	1	2
$^2\Delta$	2	2	4	3	2			75
	2	2	3	3	2	1		2
	2	2	2	3	2	2		7
	2	1	1	3	2	1	1	2
$1\,^2\Phi$	2	2	4	3	1	1		77
	2	2	3	3	1	2		3
	2	2	2	3	1	3		4
$1\,^2\Pi$	2	2	4	3	1	1		70
	2	2	4	4	0	1		8
	2	2	2	3	1	3		3
$2\,^2\Phi$	2	2	4	3	1	1		76
	2	2	2	3	1	3		4
$2\,^2\Pi$	2	2	4	3	1	1		67
	2	2	4	4	0	1		7
	2	2	3	3	1	2		3
	2	2	2	3	1	3		3
$^4\Phi$	2	2	4	3	1	1		78
	2	2	2	3	1	3		4
	2	1	3	3	1	2	1	1
$^4\Pi$	2	2	4	3	1	1		77
	2	2	2	3	1	3		4
	2	1	3	3	1	2	1	1
$^4\Delta$	2	2	4	3	0	2		78
	2	1	3	3	0	3	1	2
$^4\Sigma^+$	2	2	4	2	1	2		62
	2	2	3	4	1	1		13
	2	2	3	2	1	3		7
$^6\Sigma^+$	2	2	4	2	1	2		79
	2	2	3	2	1	3		3
$^6\Phi$	2	2	3	3	1	2		85
	2	1	2	3	1	3	1	2
	2	0	3	3	1	2	2	1
$^6\Pi$	2	2	3	3	1	2		81
	2	1	2	3	1	3	1	2
	2	0	3	3	1	2	2	1
$^6\Delta$	2	1	4	3	1	2		83
	2	1	2	3	1	4		2
	2	0	3	3	1	3	1	2

[a]Weights (in percent) are obtained from the square of the corresponding configuration interaction coefficients, configurations having weights greater than one are listed.
[b]States are listed in order of term energies within each spin multiplicity.
[c]Molecular-orbital occupancies are given in this column.

DISCUSSION

The carrier of the new bands was established on the basis of experimental evidence and by comparison with the known spectra of RuO and RuC. Both of the analyzed subbands have negligible isotopic splittings near the origin, and the splitting in the branches increases with J consistent with a 0–0 vibrational assignment. The intensity of the resolved isotopic lines appears in the approximate ratio of 2:5:3 (Fig. 2) which is proportional to the percentage abundance of the ^{100}Ru, ^{102}Ru, and ^{104}Ru isotopes [12.7%, 31.6%, and 18.7%, respectively], indicating that these bands certainly involve a molecule containing the Ru atom. The carrier of these bands, therefore, is either RuO, RuC, or RuN on the basis of the size of the B value. The spectra of RuO and RuC have been investigated previously and none of the new bands match with the previously reported RuO and RuC data. The fact that these bands appear when a trace of N_2 is added to the Ne flow and disappear when N_2 is replaced by O_2 provides experimental evidence that these bands belong to RuN. Moreover, the RuO and RuC bands involve electronic states of odd multiplicity while the new bands involve even multiplicity electronic states (six branches in each subband). The experimental evidence thus strongly supports a RuN carrier.

Our analysis shows that $C\ ^2\Pi - X\ ^2\Sigma^+$ transition of RuN is analogous to the same transition of isoelectronic RhC molecule near 1 μm.[49,50] The ground and excited state molecular

TABLE IV. Spectroscopic properties of the low-lying electronic states of RuN from MRCI *ab initio* calculations.

Spin multiplicity	State	T_0 (cm^{-1})	R_e (Å)	ω_e (cm^{-1})
2	$^2\Sigma^+$	0	1.578	1141
	$^2\Delta$	4778	1.621	1009
	$1\,^2\Phi$	10 372	1.688	868
	$1\,^2\Pi$	11 328	1.670	907
	$2\,^2\Phi$	13 337	1.653	982
	$2\,^2\Pi$	14 140	1.698	775
4	$^4\Phi$	5561	1.655	977
	$^4\Pi$	5805	1.657	967
	$^4\Delta$	15 090	1.697	917
	$^4\Sigma^+$	18 986	1.832	645
6	$^6\Sigma^+$	12 627	1.734	835
	$^6\Phi$	22 119	1.908	637
	$^6\Pi$	23 457	1.909	628
	$^6\Delta$	29 380	1.853	655

constants of RuN and RhC are very similar. For example the $X\ ^2\Sigma^+$ ground-state rotational constants for RhC are $B_0 = 0.6007\ cm^{-1}$ and $\gamma_0 = -0.067\ cm^{-1}$ compared to our values of $B_0 = 0.552\,782\,9\ cm^{-1}$ and $\gamma_0 = -0.044\,432\ cm^{-1}$ for the ground state of RuN. The $A\ ^2\Pi$ excited state of RhC has $B_0 = 0.570\,24\ cm^{-1}$ and $A_0 = 775.80\ cm^{-1}$ compared with $B_0 = 0.516\,843\,4\ cm^{-1}$ and $A_0 = 725.8064\ cm^{-1}$ for RuN. These observations indicate that the ground and excited electronic states of these two molecules share many similarities.

Since the weaker bands could not be rotationally analyzed, equilibrium constants could not be determined for RuN. It is, however, worthwhile to compare the r_0'' bond length of RuN [1.573 869(10) Å] with that of RuO [1.715 Å] and RuO [1.635 Å] The short RuN bond length is consistent with a formal triple bond between the atoms. Although the assignment of the weaker band heads of RuN is only tentative, the $\Delta G_{1/2}''$ value of 1106 cm^{-1} for RuN is higher than that for RuO (885 cm^{-1}) and for RuC (1030 cm^{-1}). Values for $\Delta G_{1/2}'' = 1040\ cm^{-1}$ and $r_0 = 1.6133$ Å were obtained for the isoelectronic RhC.[49]

For the RhC molecule two additional excited electronic states, $B\ ^2\Sigma^+$ and $C\ ^2\Sigma^+$, have been observed in the visible region and a third ($D\ ^2\Sigma^-$) state has been predicted from perturbations in the $C\ ^2\Sigma^+$ state.[65] The existence of analogous excited electronic states of RuN cannot be confirmed at present since the visible and ultraviolet regions are still to be investigated. Work in this direction will be carried out in the near future.

It is interesting to compare the calculated energy levels of RuN (see Fig. 6) with those of the isovalent FeN molecule.[43–45] In general, for RuN the quartet and, particularly, the sextet manifolds are pushed to higher energies than in FeN. Thus the low-spin states seem to be stabilized relative to high spin states for $4d$ transition metal nitrides. Within the spin manifolds the ordering of the states also changes with, in particular, the $^2\Sigma^+$ state being the ground state in RuN. The actual ground state in FeN is not well established with $^2\Delta$, $^4\Pi$, and $^6\Sigma^+$ all lying low in energy.[45] A similar comparison can be made between the energy levels of the iselectronic RuN and RhC molecules.[50] In this case the comparison is more favorable with strong similarities between the two molecules. The doublet, quartet and sextet manifolds of RuN are closer in energy than in the RhC case. The ordering of some of excited RhC states is also different with, for example, the $^2\Phi$ state of RhC lying above the first $^2\Pi$ state. It seems, however, that transition metal nitrides and corresponding isoelectronic carbides have similar electronic structure and spectroscopic properties.

There is good agreement between the *ab initio* calculations and the experimental parameters in RuN. For the ground state the calculated $r_e = 1.578$ Å and $\omega_e = 1141\ cm^{-1}$ compare very favorably with the observed $r_0 = 1.574$ Å and $\omega_e = 1122\ cm^{-1}$. For the excited $C\ ^2\Pi$ state the calculated values are $T_0 = 11\,328\ cm^{-1}$ $r_e = 1.670$ Å and $\omega_e = 907\ cm^{-1}$ while the experimental results are $T_0 = 7714\ cm^{-1}$, $r_0 = 1.628$ Å and $\Delta G_{1/2} \approx 1002\ cm^{-1}$. The relatively short RuN bond length and high vibrational frequency in the $X\ ^2\Sigma^+$ state can be explained by occupation of the strongly bonding 1π and 2σ orbitals (Fig. 7). Even the δ orbitals are bonding and the singly occupied 3σ orbital is only slightly antibonding.

The discrepancy of 3614 cm^{-1} for the term energy of the $C\ ^2\Pi$ state can be considered reasonable at the level of theory adopted in this work. The importance of the basis set size and of electron correlation in transition metal-containing molecules is well-known. The major defects of our calculations are: (i) The use of a core potential; (ii) the use of a medium-sized basis set; (iii) the neglect of relativistic effects, except the inclusion of the WB averaged contributions in the pseudo potential; and (iv) the definition of a valence space excluding the $4s$ and $4p$ orbitals of ruthenium. Some of these defects cannot easily be eliminated for a system like RuN. We believe, however, that further improvements in the *ab initio* methodology would not qualitatively change the results obtained.

CONCLUSION

We have observed an infrared electronic transition of RuN using a Fourier transform spectrometer. The bands observed near 7354 and 8079 cm^{-1} have been assigned as the 0–0 bands of the $^2\Pi_{1/2}-^2\Sigma^+$ and $^2\Pi_{3/2}-^2\Sigma^+$ subbands of the $C\ ^2\Pi - X\ ^2\Sigma^+$ transition. A rotational analysis of these two subbands has been carried for the most abundant ^{102}RuN isotopomer and principal molecular constants have been determined for the ground and excited states. The ground state of RuN has a bond length of $r_0 = 1.573\,869(10)$ Å compared with $r_e = 1.715$ Å for the ground state in the RuO consistent with a formal triple bond in RuN. We have also explored the low-lying doublet, quartet, and sextet spin manifolds by *ab initio* calculation. The present assignments are in agreement with data for the isoelectronic molecule RhC[49,50] and are also supported by our *ab initio* calculations.

ACKNOWLEDGMENTS

We thank J. Wagner, C. Playmate, and M. Dulick of the National Solar Observatory for assistance in obtaining the spectra. The National Solar Observatory is operated by the Association of Universities for Research in Astronomy, Inc.,

under contract with the National Science Foundation. The research described here was supported by funding from the NASA laboratory astrophysics program and the Petroleum Research Fund administered by the American Chemical Society. Support was also provided by the Natural Sciences and Engineering Research Council of Canada. J. Liévin thanks the ''Fonds National de Recherche Scientifique de Belgique'' (Contract FRFC 2-4551.92) for financial support.

[1] D. N. Davis, Astrophys. J. **106**, 28 (1949).
[2] H. Spinard and R. F. Wing, Annu. Rev. Astron. Astrophys. **7**, 269 (1969).
[3] M. Grunze, in *The Chemical Physics of Solid Surfaces and Heterogeneous Catalysis, Vol. 4*, edited by D. A. King and D. P. Woodruff (Elsevier, New York, 1982), p. 143.
[4] F. A. Cotton and G. Wilkinson, *Advanced Inorganic Chemistry. A Comprehensive Text*, 5th ed. (Wiley, New York, 1988).
[5] C. W. Bauschlicher, Jr., S. P. Walch, and S. R. Langhoff, *Quantum Chemistry: The Challenge of Transition Metals and Coordination Chemistry*, edited by A. Veillard, NATO ASI Ser. C (Reidel, Dordrecht, 1986).
[6] S. R. Langhoff and C. W. Bauschlicher, Jr., Annu. Rev. Phys. Chem. **39**, 181 (1988).
[7] M. Dolge, U. Wedig, H. Stoll, and H. Preuss, J. Chem. Phys. **86**, 2123 (1987).
[8] P. E. M. Siegbahn, Chem. Phys. Lett. **201**, 15 (1993).
[9] C. J. Cheetham and R. F. Barrow, Adv. High Temp. Chem. **1**, 7 (1967).
[10] K. P. Huber and G. Herzberg, *Molecular Spectra and Molecular Structure IV. Constants of Diatomic Molecules* (Van Nostrand Reinhold, New York, 1979).
[11] A. J. Merer, Annu. Rev. Phys. Chem. **40**, 407 (1989).
[12] G. J. Leigh, Science **279**, 506 (1998).
[13] Y. Nishinayashi, S. Iwai, and M. Hidai, Science **279**, 540 (1998).
[14] C. Jascheck and M. Jascheck, *The Behavior of Chemical Elements in Stars* (Cambridge University Press, Cambridge, 1995).
[15] H. Machara and Y. Y. Yamashita, Publ. Astron. Soc. Jpn. **28**, 135 (1976).
[16] D. L. Lambert and R. E. S. Clegg, Mon. Not. R. Astron. Soc. **191**, 367 (1980); Y. Yerle, Astron. Astrophys. **73**, 346 (1979).
[17] B. Lindgren and G. Olofsson, Astron. Astrophys. **84**, 300 (1980).
[18] D. L. Lambert and E. A. Mallia, Mon. Not. R. Astron. Soc. **151**, 437 (1971).
[19] O. Engvold, H. Wöhl, and J. W. Brault, Astron. Astrophys., Suppl. Ser. **42**, 209 (1980).
[20] R. T. Carter, T. C. Steimle, and J. M. Brown, J. Chem. Phys. **99**, 3166 (1993).
[21] R. S. Ram and P. F. Bernath, J. Chem. Phys. **105**, 2668 (1996); J. Mol. Spectrosc. **183**, 263 (1997).
[22] A. W. Taylor, A. S-C. Cheung, and A. J. Merer, J. Mol. Spectrosc. **113**, 487 (1985).
[23] Y. Azuma and A. J. Merer, J. Mol. Spectrosc. **135**, 194 (1989).
[24] A. G. Adam, M. Barnes, B. Berno, R. D. Bower, and A. J. Merer, J. Mol. Spectrosc. **170**, 94 (1995).
[25] O. Launila, B. Schimmelpfennog, H. Fagerli, O. Gropen, A. G. Taklif, and U. Wahlgren, J. Mol. Spectrosc. **186**, 131 (1997).
[26] R. S. Ram and P. F. Bernath, J. Chem. Phys. **96**, 6344 (1992).
[27] R. S. Ram and P. F. Bernath, J. Mol. Spectrosc. **165**, 97 (1994).
[28] R. S. Ram and P. F. Bernath, J. Mol. Spectrosc. **184**, 401 (1997).
[29] R. S. Ram and P. F. Bernath, J. Opt. Soc. Am. B **11**, 225 (1994).
[30] R. S. Ram, P. F. Bernath, W. J. Balfour, J. Cao, C. X. W. Qian, and S. J. Rixon, J. Mol. Spectrosc. **168**, 350 (1994).
[31] W. J. Balfour, J. Cao, C. X. W. Qian, and S. J. Rixon, J. Mol. Spectrosc. **183**, 113 (1997).
[32] W. J. Balfour (private communication).
[33] W. J. Balfour, C. X. W. Qian, and C. Zhou, J. Chem. Phys. **106**, 4383 (1997); **107**, 4473 (1997).
[34] E. J. Friedman-Hill and R. W. Field, J. Chem. Phys. **100**, 6141 (1994).
[35] K. Y. Jung, T. C. Steimle, D. Dai, and K. Balasubramanian, J. Chem. Phys. **102**, 643 (1995).
[36] A. J. Marr, M. E. Flores, and T. C. Steimle, J. Chem. Phys. **104**, 8183 (1996).
[37] K. L. Kunze and J. F. Harrison, J. Am. Chem. Soc. **112**, 3812 (1990).
[38] I. Shim and K. A. Gingerich, Int. J. Quantum Chem. **46**, 145 (1993).
[39] C. W. Bauschlicher, Jr., Chem. Phys. Lett. **100**, 515 (1983).
[40] S. M. Mattar, Jr., J. Phys. Chem. **97**, 3171 (1993).
[41] J. F. Harrison, J. Phys. Chem. **100**, 3513 (1996).
[42] S. M. Mattar and B. J. Doleman, Chem. Phys. Lett. **216**, 369 (1993).
[43] P. E. M. Siegbahn and M. R. A. Blomberg, Chem. Phys. **87**, 189 (1984).
[44] M. R. A. Blomberg and P. E. M. Siegbahn, Theor. Chim. Acta **81**, 365 (1992).
[45] A. Fiedler and S. Twata, Chem. Phys. Lett. **271**, 143 (1997).
[46] R. Scullman and B. Thelin, J. Mol. Spectrosc. **56**, 64 (1975).
[47] J. G. Kay, D. W. Green, K. Duca, and G. L. Zimmerman, J. Mol. Spectrosc. **138**, 49 (1969).
[48] R. Scullman and B. Thelin, Phys. Scr. **3**, 19 (1971); **5**, 201 (1972).
[49] B. Kaving and R. Scullman, J. Mol. Spectrosc. **32**, 475 (1969).
[50] H. Tan, M. Liao, and K. Balasubramanian, Chem. Phys. Lett. **280**, 423 (1997).
[51] S. R. Langhoff, C. W. Bauschlicher, L. G. M. Pettersson, and P. E. M. Siegbahn, Chem. Phys. **132**, 49 (1989).
[52] B. A. Palmer and R. Engleman, *Atlas of the Thorium Spectrum* (Los Alamos National Laboratory, Los Alamos, 1983).
[53] H.-J. Werner and P. J. Knowles, J. Chem. Phys. **89**, 5803 (1988); P. J. Knowles and H.-J. Werner, Chem. Phys. Lett. **145**, 514 (1988).
[54] H.-J. Werner and P. J. Knowles, J. Chem. Phys. **82**, 5053 (1985); P. J. Knowles and H.-J. Werner, Chem. Phys. Lett. **115**, 259 (1985).
[55] MOLPRO (version 96.4) is a package of *ab initio* programs written by H.-J. Werner and P. J. Knowles, with contributions of J. Almlöf, R. D. Amos, M. J. O. Deegan, S. T. Elbert, C. Hampel, W. Meyer, K. Peterson, R. Pitzer, A. J. Stone, P. R. Taylor, and R. Lindh.
[56] D. Andrea, U. Häussermann, M. Dolg, H. Stoll, and H. Preuss, Theor. Chim. Acta **77**, 123 (1990).
[57] A. Bergner, M. Dolge, W. Kuechle, H. Stoll, and H. Preuss, Mol. Phys. **80**, 1431 (1993).
[58] J. H. Wood and A. M. Boring, Phys. Rev. B **18**, 2701 (1978).
[59] K. Ruedenberg, M. W. Schmidt, M. M. Gilbert, and S. T. Elbert, Chem. Phys. **71**, 41 (1982); B. O. Roos in, *Advances in Chemical Physics, Ab Initio Methods in Quantum Chemistry, Part 2*, edited by K. P. Lawley (Wiley, New York, 1978), Vol. 67, pp. 399–445.
[60] E. R. Davidson, J. Comput. Phys. **17**, 87 (1975).
[61] See AIP Document No. PAPS JCPSA6-109-013839 for 3 pages of data tables. Order by PAPS number and journal reference from American Institute of Physics, Physics Auxiliary Publication Service, 500 Sunnyside Boulevard, Woodbury, NY 11797-2999. Fax: 516-576-2223, E-mail: paps@aip.org. The price is $1.50 for each microfiche (98 pages) or $5.00 for photocopies of up to 30 pages, and $0.15 for each additional page over 30 pages. Airmail additional. Make checks payable to the American Institute of Physics.
[62] J. Brown, E. A. Colbourn, J. K. G. Watson, and F. D. Wayne, J. Mol. Spectrosc. **74**, 294 (1979).
[63] M. Douay, S. A. Rogers, and P. F. Bernath, Mol. Phys. **64**, 425 (1988).
[64] C. Amiot, J. P. Maillard, and J. Chauville, J. Mol. Spectrosc. **87**, 196 (1981).
[65] A. Lagerqvist and R. Scullman, Ark. Fys. **32**, 479 (1966).